

# Recreating the Feel of the Human Chest in a CPR Manikin via Programmable Pneumatic Damping

Andrew A. Stanley\*  
Haptics Group, GRASP Lab  
Mechanical Engineering and  
Applied Mechanics Dept.  
University of Pennsylvania

Simon K. Healey†  
Haptics Group, GRASP Lab  
Mechanical Engineering and  
Applied Mechanics Dept.  
University of Pennsylvania

Matthew R. Maltese‡  
Biomechanics Research  
Dept. of Anesthesiology and  
Critical Care Medicine  
The Children's Hospital of  
Philadelphia

Katherine J. Kuchenbecker§  
Haptics Group, GRASP Lab  
Mechanical Engineering and  
Applied Mechanics Dept.  
University of Pennsylvania

## ABSTRACT

It is well known that the human chest exhibits a strong force-displacement hysteresis during CPR, a stark contrast to the non-hysteretic behavior of standard spring manikins. We hypothesize that individuals with experience performing CPR on humans would perceive a manikin with damping as more realistic and better for training. By analyzing data collected from chest compressions on real patients, we created a dynamic model that accounts for this hysteresis with a linear spring and a one-way variable damper, and we built a new high-fidelity manikin to enact the desired force-displacement relationship. A linkage attached to the chest plate converts vertical compression motions to the horizontal displacement of a set of pneumatic dashpot pistons, sending a volume of air into and out of the manikin through a programmable valve. Position and pressure sensors allow a microcontroller to adjust the valve orifice so that the provided damping force closely follows the desired damping force throughout the compression cycle. Eight experienced CPR practitioners tested both the new manikin and an identical looking standard manikin; the manikin with damping received significantly higher ratings for haptic realism and perceived utility as a training tool.

**Index Terms:** H.5.1 [Information Interfaces and Presentation]: Multimedia Information Systems—Artificial, Augmented, and Virtual Realities; H.5.2 [Information Interfaces and Presentation]: User Interfaces—Haptic I/O

## 1 INTRODUCTION

Cardiac arrest is a significant health issue. The worldwide incidence of out-of-hospital cardiac arrests ranges from 49 to 83 per 100,000 individuals per year [25, 9]. In-hospital arrests range from 1 to 5 arrests per 1,000 patients [23], and annual sudden cardiac death estimates range from 180,000 to greater than 450,000 in the United States alone [16]. Survival rates range from 2% to 7% for witnessed out-of-hospital arrests with cardiopulmonary resuscitation (CPR) administered by a bystander [15], and 15% to 20% for in-hospital arrests with CPR administered by trained professionals [23].

CPR technique has a significant effect on the patient's outcome. Uninterrupted deep chest compressions are known to be essential to survival [14, 24, 29], and even short (4 to 5 second) pauses between chest compressions cause a decrease in coronary perfusion pressure [6]. Thus, the American Heart Association (AHA) guidelines for CPR have changed over the past decade to increase the

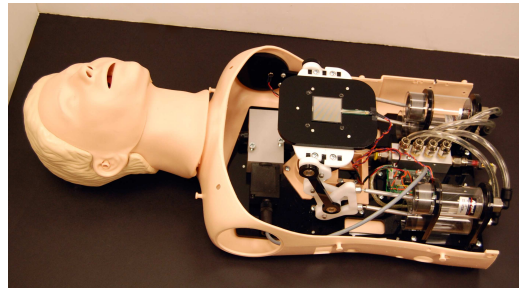


Figure 1: The CPR manikin developed in this work, shown without a chest plate or skin to reveal custom internal components.

proportion of time that chest compressions are delivered, as opposed to ventilation. For example, the 2005 guidelines increased the chest-compression-to-breath ratio from 15:2 to 30:2, and emphasized the phrase “push hard and push fast” to ensure that adequate compression rate and depth are maintained [2]. The most recent AHA guidelines ask even more of the rescuer, now increasing compression depth from “38 to 51 mm” [2] to “at least 51 mm” [8] for adults. This increased focus on chest compressions translates to a greater need to properly train CPR providers, ranging from the lay-rescuer to the medical professional.

The CPR manikin is a key tool for CPR training. Such devices have humanoid form and an internal spring or foam to enable the rescuer to practice chest compressions. Through structured courses around the world, CPR training aims to give the most inexperienced rescuer the ability to save a cardiac arrest victim. Even though it is a major cause of death, the average person has never witnessed a cardiac arrest. Thus, lay-rescuers who intervene must have had training that adequately simulated real arrest conditions.

We hypothesize that individuals with experience performing CPR on humans would perceive a manikin with carefully tuned damping as more realistic and better for training than a standard spring-based manikin. After reviewing prior work, we present the development of an advanced CPR manikin (Fig. 1) that emulates the feel of a patient's chest using a linear spring, a measurement-based haptic feedback model, and actively controlled pneumatic damping. We then describe the results of a blinded crossover study in which experienced CPR providers evaluated this manikin's simulation of one representative patient alongside a standard manikin.

## 2 BACKGROUND

Numerous electromechanical devices have been employed over the past three decades to measure compression force and depth during CPR in animals and humans. Such devices range from load cell and displacement sensors interposed between the hands of the compressor and the chest of the patient [26], to adding force and depth sensors to mechanical devices that completely replace the human compressor [27]. These experiments have revealed two important properties of the chest during CPR.

\*e-mail: astan@seas.upenn.edu

†e-mail: shealey@seas.upenn.edu

‡e-mail: maltese@email.chop.edu

§e-mail: kuchenbe@seas.upenn.edu

First, applied force increases non-linearly with displacement in adult patients [26, 11, 27], pediatric patients [18], human cadavers [13], and animal models [19, 12]. A large sample of 91 out-of-hospital patients (median age 70 years, 61 males) who received chest compressions by emergency medical personnel found that compressing the adult chest 38 mm required approximately 320 newtons (N) of force, with 2.3 to 3.3 times more force required to double the depth of the chest compression [26]. Second, the chest absorbs energy during the compression cycle. A typical single chest compression cycle in adults [3, 11], children and young adults [18], cadavers [13], and animals [19, 12] exhibits hysteretic behavior, creating a loop in the force-deflection curve.

Many studies mathematically model the chest as a spring in parallel with a dashpot, e.g., [11, 26]. With this model paradigm, linear damping coefficients have been shown to increase with depth of compression [3, 11], and they range from 71 N·s/m at compression onset to 337 N·s/m at 38 mm of chest depth. Damping coefficients also decrease by as much as 10% after 200 compression cycles [19], as shown in both human and animal studies. Maximum sternum velocity during CPR is about 0.25 meters per second [18], and thus damping forces range from 18 to 84 N, which is 6 to 26% of the total force generated by the chest (320 N @ 38 mm) reported by Tomlinson [26]. Clearly damping forces are significant.

Much of the previous research on CPR manikin design has focused on manikins that vary in stiffness [5, 21], while some more recent projects have begun to include damping in the simulation. One chest simulator models the human chest as a bilinear spring in parallel with a linear damper [28], and it creates a force-deflection curve based on this model using passive mechanical components (two linear springs and one hydraulic damper in parallel). Another project models the human chest as a progressive spring, increasing in stiffness with increasing depth, in parallel with a non-linear damper [20], using eight replaceable springs of varying progressive stiffness and a passive pneumatic damper to supply the damping force in the manikin. The constant size of the slit of the orifice in this pneumatic damper was designed to most accurately mimic the damping of the human chest between 10 mm and 30 mm of compression, but the air in the damper was noted to act more like a spring when overpressure was achieved in the cylinder.

The use of purely passive components limits one’s ability to adjust the damping characteristics of the manikin, and it also restricts the dynamic models upon which they can be based to models that behave identically during the compression and the rebound of the human chest. Thus, the goal of this research project was to build a CPR manikin that delivers haptic sensations comparable to the human chest and has the capability of adjusting its damping forces to simulate various patient and arrest characteristics.

### 3 DATA-DRIVEN MODELING OF HUMAN CHEST DYNAMICS

To streamline the manikin design process, we adopted a measurement-based approach to haptic modeling [22], aiming to create a parametric input-output model of human chest dynamics.

#### 3.1 Chest Compression Data

Force and deflection sensors (FDS) are now often built into patient monitor-defibrillators so that clinicians can receive instantaneous feedback on the quality of the chest compressions they perform on actual patients. The FDS incorporates a force sensor and an accelerometer into a small handheld device, commonly called a “puck,” that the clinician holds against the patient’s chest throughout the CPR session. By twice integrating the accelerometer signal and compensating for drift, this device provides a real-time visual display of the depth of each compression while also providing auditory feedback on compression frequency and force to encourage the clinician to more closely follow the AHA guidelines [1].

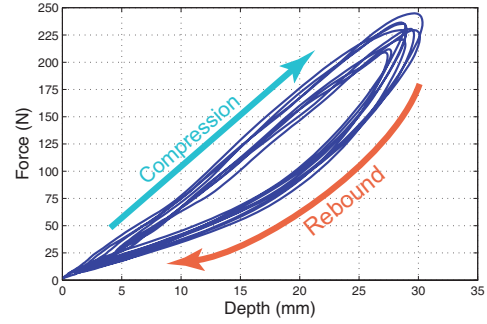


Figure 2: Force-displacement data from real chest compressions.

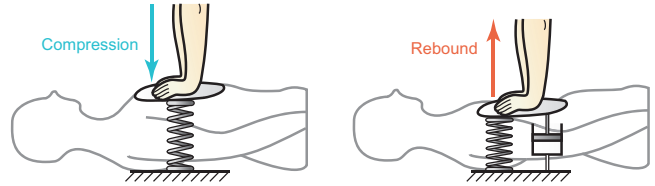


Figure 3: Dynamic chest models during compression and rebound.

FDS tools were designed to improve the quality of CPR administered by a clinician, but they also provide researchers with an opportunity to collect physical motion data that has long been inaccessible. In particular, the data recorded by CPR pucks can be analyzed to elucidate the force-deflection behavior of the patient’s chest, as demonstrated by Arbogast et al. [3]. The Laerdal Q-CPR Technology FDS has been integrated into the care of patients in the emergency room at the Children’s Hospital of Philadelphia, providing us with a large data set to consider. After examining data from many CPR incidents, we chose to focus this paper on developing methods that enable us to recreate the force-deflection characteristics of a single, representative patient.

The data used for our dynamic model came from chest compressions on a 21-year-old male patient. The raw force and position data from the puck was post-processed using the techniques of Maltese et al. [18] to remove the dynamic effects of the mattress beneath the patient. This process provided over sixty full compression cycles of force-versus-time and deflection-versus-time data upon which to base our dynamic model. A force-versus deflection plot for several compression cycles is shown in Fig. 2. The most notable feature of this force-deflection curve is the hysteresis caused by the viscoelastic nature of the human chest, indicating that a spring alone would not be a sufficient model.

#### 3.2 Dynamic Model

Each of the loops in Fig. 2 represents a single chest compression during CPR. The higher-force top half of the loop was generated by the downward compression of the clinician’s hands into the patient’s chest, and the lower-force bottom half resulted from the rebound of the chest as the clinician released. A simple mass-spring dynamic model would generate a purely linear force-deflection curve, and a mass-spring-damper model would generate a symmetric loop; however, the patient data reflects neither of these classifications. The compression into the chest looks like a linear spring, as the slope is approximately constant. In contrast, the rebound appears to include damping, which reduces the force felt and causes hysteresis. The diagrams in Fig. 3 depict the dynamic models that we propose to fit the data from the human patient; transitions between the two models occur at the top and bottom of each compression, where velocity is zero, so the transitions are smooth. Note that one must be careful in interpreting the physical significance of this model; though it fits the data well, we are not proposing that there is no dissipation during the downward

compression of the chest. Instead, we believe that the nonlinear stiffness of the chest combines with nonlinear damping to yield force-deflection curves like those shown in Fig. 2, which are well modeled by the hybrid dynamic system shown in Fig. 3.

### 3.3 Parameter Fitting

To calculate the best value for each parameter in our dynamic model, we split the data set into individual compression cycles, defining the starting point of each compression by the local minimum in the deflection versus time data. Finding each local maximum allowed us to further break each cycle into a downward compression and an upward rebound phase. The slope of each of the compression sections provides the effective linear spring stiffness. Averaging the stiffness values from all of the compression cycles gave the spring constant  $k = 7956 \text{ N/m}$ .

The linear damping coefficient and the mass term were fit based on the data from the rebound phases. For each data point, we calculated the difference between the predicted spring force and the actual force exhibited by the human chest. This vector of residual forces represents the downward damping force and the inertia of the chest during the rebound. We performed a least-squares fit between these forces and the corresponding velocity and acceleration of the chest at each point, found by differentiating and smoothing the deflection-versus-time data. The results were  $b = 217 \text{ N}\cdot\text{s/m}$  and  $m = 2.39 \text{ kg}$ . It is notable that the inertial forces of the chest movement are almost negligible in comparison to the spring and damping forces, consistent with findings of Bankman et al. [4].

We verified our dynamic model by evaluating it on the deflection data from the actual chest compressions and comparing the output to the actual forces. We also compared this time history to a simulation of the forces that the model would produce if the damping component was not included, as is done in standard spring-based manikins. Fig. 4 shows the results of these tests. Plotting the residual error force between each of these models and the actual force data highlights the importance of including the damping component in the dynamic model, as it reduces the maximum force error from over 60 N to less than 10 N.

## 4 MANIKIN DESIGN

Once satisfied with the model, we needed to create a haptic device that could accurately render the model's dynamics, which include a large spring force and a strong one-way damper. Furthermore, we aimed to create a system that could be reprogrammed to emulate the feel of many different patients, not just the one modeled in the previous section. Rather than creating a fully custom manikin, we opted to modify the internal components of an existing manikin so that we could more easily compare the unique aspects of our design to the state of the art.

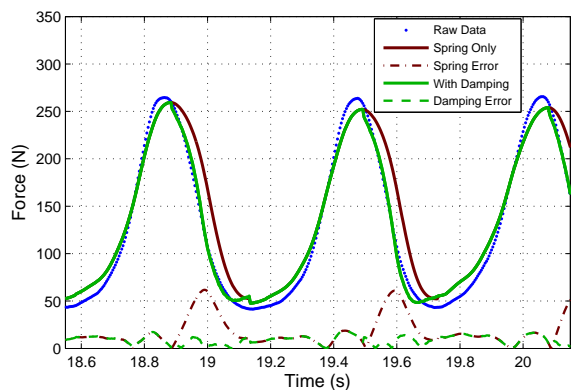


Figure 4: Adding one-way linear damping to the simple spring model reduces modeling errors on the rebound.

## 4.1 Actuator Selection

Many data-driven haptic rendering systems commonly rely on backdrivable DC-motor-based devices to record and replay the desired sensations [22]. However, the forces exhibited by the human chest during CPR are orders of magnitude higher than what any commercial haptic device can provide, requiring a novel method for accurate rendering. While an active electromechanical system like a DC motor or a solenoid might provide the most controllable force output, such a device would need to be very large to recreate the forces that a human chest exerts when fully compressed to its greatest depth (600 N). Even if such an actuator could fit inside the manikin, it would have very high inertia and would generate excessive heat. Similarly, we rejected the option of using a cable transmission to gear down a large DC motor because its effective inertia would be too high to represent the low mass of the chest.

After prototyping many options, we ultimately chose to actuate our manikin using passive mechanical elements (a coil spring and a pneumatic damper) with active control over the damping component. We selected a linear spring that closely matches  $k$ , the stiffness calculated from the 21-year-old male patient's data. To enable simulation of a variety of patient ages and physiques, we designed the manikin to enable easy spring replacement.

For damping, a set of four customized Airpot 2K444 dashpots are pneumatically connected through a manifold. These dashpots have an internal diameter of 4.45 cm, and they were customized with 7.5-cm stroke lengths. A tube from the manifold leads to one port of a Festo MPYE5-3 1/4-10 proportional valve, allowing adjustment of the effective combined orifice of the dashpot cylinders. The graphite pistons of the dashpots slide with minimal friction inside the glass cylinders, preventing any unwanted haptic sensations from interfering with the feel of the compression cycles. The damping force at any point during a compression is equal to the gauge pressure inside the dashpot cylinders multiplied by the combined cross-sectional areas of the pistons (Fig. 5); this calculation dictated the need for four dashpots acting in parallel.

Analog readings from a potentiometer and a Honeywell ASDX030A24R pressure transducer measure the vertical deflection of the chest and the pressure inside of the dashpot cylinders, respectively. Based on these readings, an AVR microcontroller sends a pulse-width-modulation (PWM) voltage to the valve; after being smoothed by a first-order low-pass analog filter set at 160 Hz, this command signal adjusts the cross-sectional area of the valve's orifice. This scheme, explained in further detail below, controls the damping force from the dashpots to match the desired damping force from the dynamic model at each point in the cycle.

Beyond its low moving mass and its ability to achieve force magnitudes greater than a similarly-sized active electromechanical actuator, a programmable passive pneumatic actuator also enables easy reprogramming of the manikin to create a wide range of linear and nonlinear damping characteristics, to simulate a tremendous variety of patients. Damping constants decrease by as much as 10% after 200 compression cycles [19] in real human resuscitations and ani-

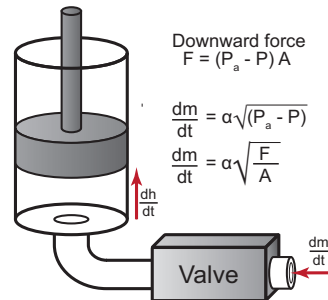


Figure 5: Diagram of one cylinder and the controllable valve.

mal experiments; thus our flexible design will allow us to simulate more sophisticated damping features in future studies. A simple passive element, such as a one-way pneumatic or hydraulic damper, would not allow such adjustments.

## 4.2 Mechanical Design

We constructed our manikin by replacing the internal components of an existing manikin, a Laerdal Medical Resusci Anne Torso Skillreporter. This model of manikin is currently used at the Children’s Hospital of Philadelphia for training both new and experienced CPR practitioners. We use its chest plate and spring support bracket to hold the spring in the center of the manikin, but we replaced all of its other internal components. Fig. 1 shows a photograph of our final manikin prototype with the chest plate and skin removed for better visibility. All custom-designed pieces were cut out of acrylic and medium-density fiberboard using a laser cutter. Beyond the shape of the manikin shell, limiting the height of the chest to realistic values represented the main mechanical constraint. The chest plate needs space to be able to move approximately 75 mm downward to avoid bottoming out when a user surpasses the AHA guidelines for compression depth, and the entire manikin must be shorter than approximately 180 mm in the uncompressed state to avoid appearing abnormally large.

This height constraint prevented us from orienting the dashpots vertically, so we designed a system to convert the vertical motion of the chest plate into the horizontal motion of the dashpot pistons. Our early prototypes employed a low friction push-pull cable for this purpose, connecting the bottom of the chest plate down through the spring, through a right-angle turn, and over to the tops of the horizontally oriented dashpot rods. Because the dynamic model includes no damping during the downward compression, when the cable is in compression, we hoped the push-pull cable would function well throughout each cycle. However, the inertial forces required to push the dashpot pistons to the bottoms of the cylinders at the 100-beat-per-minute pace of CPR proved enough to cause the cable to buckle occasionally, so we sought another solution.

Our final manikin uses two parallel copies of a custom linkage to mechanically re-orient the motion of the chest plate. Fig. 6 depicts the linkage design; the two copies of the linkage are positioned on either side of the spring, and each one connects to two dashpot rods. A right-isosceles triangle mounts rigidly to a support connected to the base plate and rotates about its right angle vertex, maintaining the ratio of vertical to horizontal motion. The lengths of the links connecting this triangle to the chest plate and the dashpot rods were dictated by the space constraints of the manikin. The fourth link connects these two links together to maintain an approximately constant orientation of the dashpot rod connection. The placement of each end of this fourth link was optimized in software using a brute-force search that sought to keep the two dashpot rods as parallel to each other as possible throughout the device’s entire range of motion. Miniature sleeve bearings press-fitted into each linkage joint connect the links with minimal friction.

A long-stemmed rotational potentiometer mounts into one of the triangle link supports with its stem glued into the center of the corresponding sleeve bearing. The potentiometer is wired in a voltage divider configuration, so the microcontroller can measure the angular orientation of the triangular link as user presses on the chest plate. This angle is converted to the vertical displacement of the chest plate using kinematics. A rectangular force sensing resistor

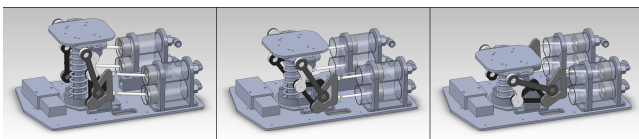


Figure 6: The manikin’s linkage moving through a compression cycle.

(Interlink 406 FSR, 3.8 cm × 3.8 cm), also used in a voltage divider circuit, is located on top of the chest plate to sense whether the user has sufficiently released pressure on the chest between compressions, as directed by AHA guidelines [8].

Space constraints dictated the remaining mechanical design choices. The pressure transducer is mounted to a spare port in the manifold and is used to measure the pressure in the dashpot cylinders. The manifold is located between the dashpots next to the circuit board, and the valve fits next to the spring near the neck of the manikin. An AC-to-DC power converter plugs into a plate in the shoulder of the manikin, next to a serial communication port that the microcontroller can use to send real-time data to a computer.

## 4.3 Valve Control

One of the major challenges of using pneumatic damping to administer precise forces in a haptic device arises from the fact that air is a compressible fluid. As a consequence, a pneumatic damper cannot achieve a constant damping coefficient simply by holding a constant orifice size. Unlike a hydraulic damper, where the flow through the orifice changes linearly with the velocity of the pistons because the liquid is incompressible, the flow rate through the orifice of a pneumatic damper changes with the pressure difference between the air inside the cylinders and the ambient air. This pressure difference relates only indirectly to the velocity of the pistons, depending also on many other factors in the state of the system. These complicating factors are balanced by the benefits of very low moving mass and wide dynamic range. We achieved precise force output with pneumatic damping by creating a closed-loop controller based on a dynamic model of the air-actuation system.

As the manikin chest moves, the microcontroller differentiates and low-pass filters the potentiometer signal to calculate the vertical velocity. If the chest is in the downward compression phase, the valve opens to minimize damping; otherwise, the chest is moving upward, and the microcontroller calculates the desired damping force based on the dynamic model of the human chest rebound described in Section 3. We tuned both analog and digital filters of the potentiometer signal to provide a suitable velocity estimate. Specifically, we needed to prevent unintended openings of the valve during the rebound, which cause the pressure inside the dashpots to “pop” back to ambient, while also maintaining a quick closure of the valve as soon as the chest enters the rebound phase.

The valve controls necessary to achieve a desired damping force required a more in-depth analysis of the dynamics of variable air damping. We use  $P_a$  for ambient air pressure,  $P = P_a - F/A$  for absolute pressure of the air inside the cylinders (Fig. 5),  $V = Ah$  for cylinder volume, and  $T$  for cylinder temperature. We aim to estimate the change in pressure that the moving pistons create, so we begin by rewriting the ideal gas law ( $PV = mRT$ ) in terms of the height of the pistons,  $h$ , and the downward damping force,  $F$ , based on the conventions shown in Fig. 5.

$$\left(P_a - \frac{F}{A}\right) (Ah) = mRT \quad (1)$$

We differentiate this expression with respect to time to allow us to model the dynamics of the system.

$$P_a A \cdot \frac{dh}{dt} - \frac{dF}{dt} \cdot h - F \cdot \frac{dh}{dt} = \frac{dm}{dt} \cdot RT \quad (2)$$

We employed an isothermal assumption ( $dT/dt = 0$ ) because the pressure changes due to temperature are much smaller than those due to the moving pistons, and a feedback compensator can sufficiently counteract this error. As the chest plate rises, the pistons move away from the orifice, and the air inside the cylinders stretches to create a partial vacuum, exerting a downward force on the chest plate.

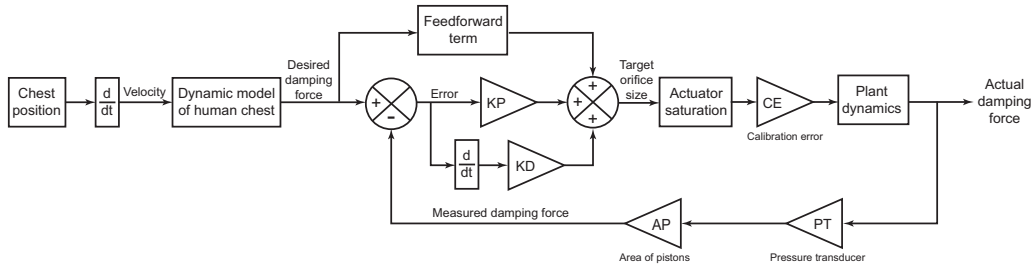


Figure 7: Controller block diagram.

The mass flow rate of air into the cylinders is proportional to the square root of the difference in pressure between the two sides of the orifice [10]. The proportionality is expressed using a valve constant,  $\alpha$ , that relates to the size and shape of the orifice.

$$\frac{dm}{dt} = \alpha \sqrt{P_a - P} \quad (3)$$

We combine all of these equations and solve for  $\alpha$  to provide the feed-forward term in the system controller, depicted by the block diagram in Fig. 7.

$$\alpha = \frac{\left( (P_a A - F) \cdot \frac{dh}{dt} - \frac{dF}{dt} \cdot h \right) \sqrt{A}}{RT \sqrt{F}} \quad (4)$$

Solving this equation for  $\frac{dF}{dt}$  allows simulation of the system.

$$\frac{dF}{dt} = \frac{(P_a A - F) \cdot \frac{dh}{dt} - \alpha RT \sqrt{\frac{F}{A}}}{h} \quad (5)$$

The feed-forward term represents the controller's best estimate of the valve orifice necessary to provide the desired damping force throughout the rebound based only on the velocity of the chest and the previous desired force. In an ideal system where the desired damping force had been perfectly achieved in the previous time step, a well calibrated feed-forward control scheme would suffice to track the desired force. However, our system included a number of factors, even beyond calibration, that necessitated the inclusion of a feedback compensator to improve tracking of the desired force.

We built a Simulink model to help analyze the dynamic effects of our system and determine the type of compensator to include in the valve controls. In addition to the feed-forward term and the plant dynamics, this model also simulated the effects of adding a proportional-derivative (PD) feedback compensator, calibration error, and actuator saturation. The actuator in this system is limited in the fact that the valve can open or close only to certain extents: the system still has some leakage even when the valve is completely closed, and the flow is still somewhat restricted when the valve is completely open.

By running the full dynamic model with position data from real CPR compressions, we compared the simulated system's force output to the actual force data from the patient. This simulation enabled us to tune the PD compensator's gains to achieve good tracking before implementing it on the actual manikin. The simulation also demonstrated an effect that the damping force does not match the desired damping at the very beginning of each rebound; this occurs because the air inside the dashpots starts at or above ambient pressure and, even with the valve completely closed, the pistons need to move a certain distance before a negative pressure can be achieved. Increasing the number of dashpots or the diameter of the dashpot pistons would reduce this effect. While the simulation provided a good starting point for tuning the PD gains, the final gain values were further tuned on the real system to achieve good force tracking.

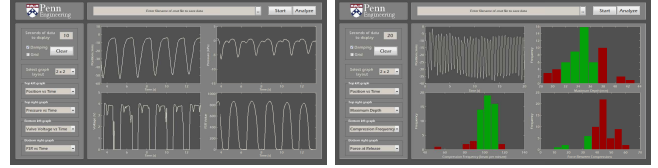


Figure 8: Screenshots from the GUI.

#### 4.4 Graphical User Interface

In addition to enabling the microcontroller to specify the damping force, the manikin's sensors also present an opportunity to give the user real-time feedback as he or she performs chest compressions. If the manikin is connected to a computer through the serial communications port in its shoulder, the microcontroller sends sensor and calculation data at a rate of 40 Hz. Our custom graphical user interface (GUI) in MATLAB allows the user to see up to four plots in real time. The user chooses between showing position, pressure, valve voltage, and FSR readings versus time. Further customization options include changing the number of seconds of past data to display, saving the data from a simulation, and starting or stopping a simulation at any time.

At the end of each simulation, the user can choose to analyze his or her performance against the AHA guidelines for CPR chest compressions. Histograms analyze the depth and frequency of the compressions in the simulation as well as whether the user adequately released pressure from the chest plate between compressions. The histogram bins are color-coded to indicate which compressions fell within compliance of the AHA guidelines. Fig. 8 shows two screenshots from the GUI, including the real-time display of data and the post-training histogram analysis.

### 5 SYSTEM EVALUATION

While engineering tests indicated that our new manikin successfully tracks the desired damping force throughout both phases of chest compression, further testing was necessary to evaluate the quantitative and qualitative success of the manikin at recreating the feel of a human chest. We therefore conducted a human subject experiment for expert CPR practitioners to test our manikin alongside a standard spring-based manikin. The University of Pennsylvania Institutional Review Board approved all study procedures under protocol 814220 with a cooperative agreement with the Institutional Review Board of the Children's Hospital of Philadelphia.

#### 5.1 Methods

We designed the study for individuals who perform chest compressions as a regular part of their clinical duties. To match the demographic upon which we based our dynamic model, we specifically sought subjects with experience administering CPR to males in their early twenties. Recruitment efforts focused on employees at both the Children's Hospital of Philadelphia and the Hospital of the University of Pennsylvania. A total of eleven clinicians volunteered to participate in this study over the span



Figure 9: Experimental setup for the study.

of two weeks; none were affiliated with the research team. All subjects had performed CPR on patients as a part of their job for at least three years. The experiences of the first three participants elucidated several issues with the initial implementation of our manikin, particularly with ensuring a fast start to the damping force when the subject was delivering 100 compressions per second, so we reworked several components before restarting the study. We classify these first three participants as a pilot study, leaving eight subjects to analyze as part of the official study data.

After giving informed consent and completing a demographic survey, subjects were instructed to perform at least twenty seconds of chest compressions on each of the manikins, with a short break between the two sets. Subjects were asked to follow the AHA chest-compression guidelines and to focus on the physical response of the manikin. Subjects completed both sessions of compressions using an FDS puck, and the attached defibrillator provided them with standard verbal coaching and visual feedback of compression rate, depth, leaning and duty cycle. As shown in Fig. 9, the manikins were positioned side by side on a table. Half of the subjects performed compressions on our manikin first, while the other half first used the standard spring manikin. The two manikins were both dressed in t-shirts and were presented to look as similar as possible, aided by the fact that our manikin is built into the same shell and skin as the standard manikin. The experimenters referred to the two as Manikin A and Manikin B, to further avoid biasing subjects.

After completing the two sets of chest compressions, subjects were presented with two identical surveys and asked to evaluate each of the manikins separately. During this time, subjects were permitted to press on either manikin as much as they desired to help them respond to the questions more accurately. The first five questions asked subjects to rate the realism and training efficacy of the specified manikin on a visual analog scale; each question was followed by a horizontal line, and the subject made a slash at the point that corresponded to the level of their answer between the two extremes. The last three questions gave subjects a free-response opportunity to note any human chest characteristics that the manikin successfully or unsuccessfully recreated, along with any other comments or suggestions about the manikin.

We used the FDS puck and the defibrillator to collect force and position data from all of the CPR sessions in the study. As this is the same tool used to collect the original data in this study, it allows easy and unbiased comparison of the force-deflection characteristics of the two tested manikins. It also provided us with the opportunity to evaluate whether the differences in the physical feel of the two manikins affected the way the clinicians performed chest compressions, as compared to the AHA guidelines.

## 5.2 Results

We statistically analyzed the data using the method of within-subject analysis of variance (ANOVA) with manikin type as the only experimental factor, using  $\alpha = 0.05$  to determine significance. We calculate the size of significant effects using the  $\eta^2$  method.

Figure 10 shows box plots for the five ratings that each subject completed for each manikin. The manikin with programmable

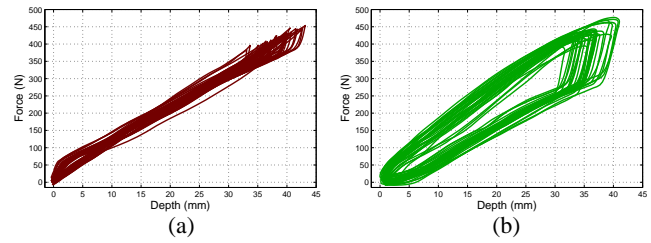


Figure 11: Sample force-deflection curves recorded during the study on the (a) standard manikin and (b) manikin with active damping. The standard manikin displays a linear relationship, while the manikin with damping has strong hysteresis on the rebound, as we intended.

damping achieved higher median ratings than the standard manikin for all five questions, and these differences achieved statistical significance for three of the questions. The manikin with programmable damping received a significantly higher rating for how well it recreates the feel of a human chest during CPR ( $F(1,15) = 30.90$ ,  $p = 0.000074$ ,  $\eta^2 = 0.6861$ ), a significantly higher rating for how well it would prepare a trainee to be familiar with the feel of performing compressions on a real patient ( $F(1,15) = 7.28$ ,  $p = 0.00173$ ,  $\eta^2 = 0.3423$ ), and a significantly higher rating for whether learning CPR on the manikin would improve the quality of chest compressions performed on actual patients ( $F(1,15) = 5.51$ ,  $p = 0.0342$ ,  $\eta^2 = 0.2823$ ). The data trended toward but did not achieve statistical significance regarding how useful a tool the manikin would be for experienced users to practice between CPR administrations ( $F(1,15) = 2.25$ ,  $p = 0.1556$ ) and for how well the manikin simulates the physical effort and fatigue associated with administering CPR ( $F(1,15) = 2.88$ ,  $p = 0.1119$ ).

We analyzed the average peak depth, peak force, and compression frequency data recorded from the FDS puck, and it did not show any statistically significant differences between the two manikins. However, the force-deflection curves that the two manikins generated did contain noticeable differences in their shapes, as seen in the representative example shown in Fig. 11.

## 5.3 Discussion

While a much larger study would be needed to test whether a certain manikin actually improves CPR performance, our subject pool of eight clinicians significantly preferred the programmable damping for increasing the biofidelity of the manikin. Furthermore, they thought it would more effectively prepare a new trainee for the feeling of the human chest. In a broader context, the results from Question 5 are particularly significant given the findings of a recent study that analyzed the survival rate of over 5,000 cases of out-of-hospital cardiac arrest based on the type of CPR performed by a bystander [7]. When the bystander performed standard CPR with ventilation, the survival rate was 7.9%, but this rate rose to 13.3% when the bystander performed chest-compression-only CPR. Our finding that clinicians believe that training on a manikin with programmable damping would improve the quality of chest compressions performed on actual patients indicates that manikins like this could increase the out-of-hospital cardiac arrest survival rate even further. At the very least, the clinicians' unanimous agreement that the programmable damping increased the haptic realism of the manikin illustrates the merits of our measurement-based approach to haptic modeling. It also shows that we successfully achieved our desired force-deflection relationship without adding any extraneous haptic artifacts that could interfere with the user experience.

We were surprised to find that the data did not reach statistical significance regarding how well each manikin simulates the physical effort and fatigue of CPR. Many of the clinicians consulted during the manikin design and some of the clinicians in the user study feel that a spring manikin does not fatigue the user as much as a real human chest because it "snaps back faster than a human"

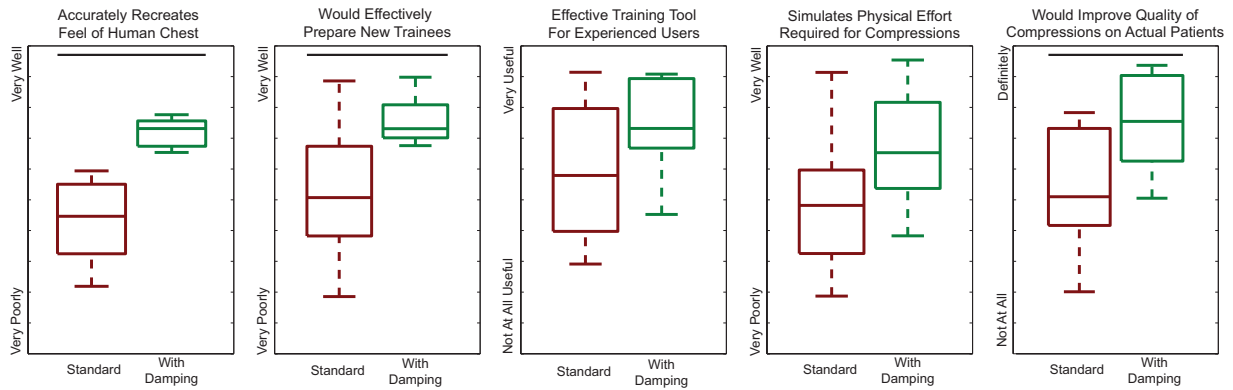


Figure 10: Box plots of the results from the survey. The line shows the median, the box shows the span of the second and third quartiles, and the whiskers show the full range of the data. The lines above denote statistical significance in the difference of the means.

and helps push the user back up on the rebound. Seven of the eight subjects rated the manikin with programmable damping higher on this continuum, but the dissenting subject noted in the free response that the standard manikin seemed stiffer, making it harder to deliver compressions, and thus rated it higher for recreating the physical effort of real compressions. However, the two manikins use springs of almost identical stiffness, so this difference was only true in perception, perhaps as an effect of the order in which this subject tested the two manikins. The force-deflection curves from the puck data clearly show more hysteresis on the manikin with programmable damping from the slower recoil. The damping absorbs energy from the user, indicating those compressions should require more effort.

Many subjects used the free-response questions to explain differences between the quantitative ratings of the manikins. In the traits that the standard manikin recreates, one user noted that it felt like a “sick chest [because it was] easy to compress.” Many users felt that the standard manikin did “not have the same recoil that [a] regular patient has” or that the “pressure on [the] rebound” seemed unrealistic. Almost all subjects specifically noted the chest recoil as a feature that our manikin successfully recreates. Both manikins received praise for their size, shape and anatomical models. One complaint described the sounds of compressions as either distracting or not typical of real compressions on both manikins. The only other negative comment written about the manikin with programmable damping was that the “skin and bones don’t feel quite like skin and bones.” Several additional comments suggested potential new features, as discussed below.

## 6 CONCLUSION

We have developed a new manikin chest that uses measurement-based haptic modeling and adjustable pneumatic damping to improve the haptic realism of CPR training. Force-deflection data from a 21-year-old male CPR patient provided the basis for the derived dynamic model of the human chest; the combination of a linear spring with a one-way damper captures the main trends in the data. Our system actively adjusts the orifice of a valve connected to four pneumatic dashpots to provide damping forces that continuously match the dynamic model. A mechanical linkage converts the vertical motion of the chest into horizontal motion of the dashpot pistons to fit within the size constraints of the manikin. A user study with clinicians experienced in administering CPR to real patients helped test the basic functionality and evaluate the biofidelity and potential added value of the system. Subjects overwhelmingly preferred the new manikin over the standard manikin, and they provided many useful comments for continued progress on this project.

Several potential improvements to this manikin and ideas for additional features open the door for future work in this area. Selecting a different valve or adding sound insulation might reduce the noise generated by the manikin during use. Several clinicians

noted that the human chest tends to deform over the course of very long CPR administrations, essentially losing the ability to return to its original height. This effect could possibly be simulated even with the manikin’s current hardware by increasing the damping coefficient during the rebound over the course of a long simulation. Another possible method for recreating this effect would involve tracking the number of chest compressions in a simulation and setting a threshold height that would lower slightly with each compression; the microcontroller could completely close the valve when the chest plate reached this height to prevent it from bouncing back any higher. Verifying that either of these approaches could accurately simulate the wearing down of a human chest would require a dynamic model based on many more compressions than were analyzed for this project.

A future phase of this research could also focus on simulating specific events that can occur during CPR. The feeling of a patient’s rib breaking or of the patient starting to gasp for air can easily startle the person performing CPR and lead them to momentarily stop performing CPR, jeopardizing the patient’s survival chances. Several clinicians in the study noted that neither manikin could recreate these physical events. Simulation of these tactile sensations likely requires further exploration of event-based haptics, which expands position-force rendering to include the high-frequency accelerations experienced during impacts and other events [17]. Replaying these vibrations has proven beneficial increasing the realism of other haptic interactions, but such an approach has not yet been applied to chest compressions. The most challenging aspect of this project phase would probably be in collecting recordings of relevant events from real CPR administrations.

The ability to reprogram a manikin chest to simulate a variety of patient age ranges and physiques without any mechanical alterations would represent another valuable feature to develop in a CPR training tool. While the damping component of our manikin can be adjusted without replacing any physical components, one must replace the spring to adjust the overall stiffness of the chest. With the infrastructure in place in this manikin, it may also be possible to use the air in the dashpots as a programmable, adjustable spring. Assuming the spring inside the manikin is as weak, or weaker, than the stiffness of the chest for a given simulation, the dashpots could add additional stiffness by restricting the flow out of the cylinders during the downward motion, causing the air to compress and add an upward force component. The same control scheme we implemented to achieve a desired damping force during the rebound could feasibly be implemented to achieve a desired spring force during the compression.

Finally, reducing the cost and simplifying the design of this manikin would likely prove necessary before standard deployment. An extensive human subject study would also be required to test the hypothesis that high-fidelity chest simulation will improve per-

formance in CPR administration. Compiling simulation data over time for a set of users, and using the performance of a separate set of users trained on conventional manikins as a control, this phase of the research would focus on statistical analysis of the significance of any changes in technique over a much longer study period. Quantification of the transfer of skills from simulation to real practice, while difficult to test, embodies an important step in justifying the additional costs of this manikin or of any other high-fidelity haptic clinical simulation.

## ACKNOWLEDGEMENTS

The authors thank Michael Boyle, Nihar Dharamsey, and Nihar Naik for helping create an earlier prototype of the manikin; Dana Niles and Vinay Nadkarni for sharing their expertise on CPR; Laerdal Medical for donating the manikins; Airpot Corporation for donating the dashpots and providing engineering guidance; Bruce Kothmann and Robert Jeffcoat for design advice; and all of the clinicians who volunteered their time to participate in the study.

## REFERENCES

- [1] B. S. Abella, D. P. Edelson, S. Kim, E. Retzer, H. Myklebust, A. M. Barry, N. O'Hearn, T. L. Hoek, and L. B. Becker. CPR quality improvement during in-hospital cardiac arrest using a real-time audiovisual feedback system. *Resuscitation*, 73(1):54–61, 2007.
- [2] American Heart Association. Part 4: Adult basic life support: American Heart Association guidelines for cardiopulmonary resuscitation and emergency cardiovascular care. *Circulation*, 112(Supplement):IV–20–IV–34, 2005.
- [3] K. B. Arbogast, M. R. Maltese, V. M. Nadkarni, P. A. Steen, and J. B. Nysaether. Anterior-posterior thoracic force-deflection characteristics measured during cardiopulmonary resuscitation: Comparison to post-mortem human subject data. *Stapp Car Crash Journal*, 50:131–145, November 2006.
- [4] I. N. Bankman, K. G. Gruben, H. R. Halperin, A. S. Popel, A. D. Guerci, and J. E. Tsitlik. Identification of dynamic mechanical parameters of the human chest during manual cardiopulmonary resuscitation. *IEEE Transactions on Biomedical Engineering*, 37(2):211–217, 1990.
- [5] M. A. Baubin, H. Gilly, A. Posch, A. Schinnerl, and G. A. Kroesen. Compression characteristics of CPR manikins. *Resuscitation*, 30(2):117–126, 1995.
- [6] R. Berg, A. Sanders, K. Kern, R. Hilwig, J. Heidenreich, M. Porter, and G. Ewy. Adverse hemodynamic effects of interrupting chest compressions for rescue breathing during cardiopulmonary resuscitation for ventricular fibrillation cardiac arrest. *Circulation*, 104(20):2465–2470, 2001.
- [7] B. J. Bobrow, D. W. Spaite, R. A. Berg, U. Stolz, A. B. Sanders, K. B. Kern, T. F. Vadeboncoeur, L. L. Clark, J. V. Gallagher, J. S. Stapczynski, F. LoVecchio, T. J. Mullins, W. O. Humble, and G. A. Ewy. Chest compression-only CPR by lay rescuers and survival from out-of-hospital cardiac arrest. *Journal of the American Medical Association*, 304(13):1447–1454, 2010.
- [8] J. M. Field and M. F. Hazinski et al. Part 1: Executive summary: 2010 American Heart Association guidelines for cardiopulmonary resuscitation and emergency cardiovascular care. *Circulation*, 122(Supplement 3):S640–S656, 2010.
- [9] M. Fries, S. Beckers, J. Bickenbach, M. Skorning, S. Krug, E. Nilson, R. Rossaint, and R. Kuhlen. Incidence of cross-border emergency care and outcomes of cardiopulmonary resuscitation in a unique european region. *Resuscitation*, 72:66–73, 2007.
- [10] D. W. Green and R. H. Perry, editors. *Perry's Chemical Engineers' Handbook*. McGraw-Hill, 2008.
- [11] K. G. Gruben, A. D. Guerci, H. R. Halperin, A. S. Popel, and J. E. Tsitlik. Sternal force-displacement relationship during cardiopulmonary resuscitation. *Journal of Biomechanical Engineering*, 115(2):195–201, 1993.
- [12] K. G. Gruben, H. R. Halperin, A. S. Popel, and J. E. Tsitlik. Canine sternal force-displacement relationship during cardiopulmonary resuscitation. *IEEE Transactions on Biomedical Engineering*, 46(7):788–96, 1999.
- [13] R. Kent, C. R. Bass, W. Woods, C. Sherwood, N. J. Madeley, and R. Salzar. Muscle tetanus and loading condition effects on the elastic and viscous characteristics of the thorax. *Traffic Injury Prevention*, 4:297–314, 2003.
- [14] K. B. Kern, R. W. Hilwig, R. A. Berg, A. B. Sanders, and G. A. Ewy. Importance of continuous chest compressions during cardiopulmonary resuscitation. *Circulation*, 105:645–649, 2002.
- [15] T. Kitamura, T. Iwami, T. Kawamura, K. Nagao, H. Tanaka, R. Berg, and A. Hiraide. Time-dependent effectiveness of chest compression-only and conventional cardiopulmonary resuscitation for out-of-hospital cardiac arrest of cardiac origin. *Resuscitation*, 82(1):3–9, 2011.
- [16] M. H. Kong, G. C. Fonarow, E. D. Peterson, A. B. Curtis, A. F. Hernandez, G. D. Sanders, K. L. Thomas, D. L. Hayes, and S. M. Al-Khatib. Systematic review of the incidence of sudden cardiac death in the united states. *Journal of the American College of Cardiology*, 57:794–801, 2011.
- [17] K. J. Kuchenbecker, J. P. Fiene, and G. Niemeyer. Improving contact realism through event-based haptic feedback. *IEEE Transactions on Visualization and Computer Graphics*, 12(2):219–230, March/April 2006.
- [18] M. R. Maltese, T. Castner, D. Niles, A. Nishisaki, and S. Balasubramanian. Methods for determining pediatric thoracic force-deflection characteristics from cardiopulmonary resuscitation. *Stapp Car Crash Journal*, 52:1–23, 2008.
- [19] A. Neuraeter, J. Nysaether, J. Kramer-Johansen, J. Eilevstjønn, P. Paal, H. Myklebust, V. Wenzel, K. H. Linder, W. Schmölz, M. Pytte, P. A. Steen, and H.-U. Strohmenger. Comparison of mechanical characteristics of the human and porcine chest during cardiopulmonary resuscitation. *Resuscitation*, 80:469–469, 2009.
- [20] J. B. Nysaether, E. Dorph, I. Rafoss, and P. A. Steen. Manikins with human-like chest properties—a new tool for chest compression research. *IEEE Transactions On Biomedical Engineering*, 55(11):2643–2650, November 2008.
- [21] S. Ødegaard, J. Kramer-Johansen, A. Bromley, H. Myklebust, J. Nysaether, L. Wik, and P. A. Steen. Chest compressions by ambulance personnel on chests with variable stiffness: Abilities and attitudes. *Resuscitation*, 74(1):127–134, 2007.
- [22] A. M. Okamura, K. J. Kuchenbecker, and M. Mahvash. Measurement-based modeling for haptic rendering. In M. Lin and M. Otaduy, editors, *Haptic Rendering: Algorithms and Applications*, chapter 21, pages 443–467. A. K. Peters, May 2008.
- [23] C. Sandroni, J. Nolan, F. Cavallaro, and M. Antonelli. In-hospital cardiac arrest: incidence, prognosis and possible measures to improve survival. *Intensive Care Medicine*, 33:237–245, 2007.
- [24] Y. Sato, M. H. Weil, and S. Sun et al. Adverse effects of interrupting precordial compression during cardiopulmonary resuscitation. *Critical Care Medicine*, 25:733–736, 1997.
- [25] T. Shiraki, K. Osawa, H. Suzuki, M. Yoshida, N. Takashi, K. Takeuchi, M. Tanakaya, K. Kohno, and D. Saito. Incidence and outcomes of out-of-hospital cardiac arrest in the eastern part of Yamaguchi Prefecture. *International Heart Journal*, 50:489–500, 2009.
- [26] A. E. Tomlinson, J. Nysaether, J. Kramer-Johansen, P. A. Steen, and E. Dorph. Compression force-depth relationship during out-of-hospital cardiopulmonary resuscitation. *Resuscitation*, 72(3):364–70, 2007.
- [27] J. E. Tsitlik, M. L. Weisfeldt, N. Chandra, M. B. Efron, H. R. Halperin, and H. R. Levin. Elastic properties of the human chest during cardiopulmonary resuscitation. *Critical Care Medicine*, 11(9):685–92, 1983.
- [28] X. Xinwu, T. Feng, S. Qiuming, W. Zheng, N. Aijuan, and H. Mingxi. A simulator of human chest that simulated force-sternal displacement relationship during cardiopulmonary resuscitation. In *Proc. IEEE International Conference on Bioinformatics and Bioengineering*, pages 1–4, 2009.
- [29] T. Yu, M. Weil, and W. Tang et al. Adverse outcomes of interrupted precordial compression during automated defibrillation. *Circulation*, 106:368–372, 2002.